CERN-LCGAPP-2008-01
November 21, 2008
Version 1.0

Hadronic Shower Shape Studies in GEANT4 : Update

J. Apostolakis[1], G. Folger[1], V. Grichine[1,2], A. Howard[1], V. Ivanchenko[1,3], M. Kosov[1,4], A. Ribon[1], V. Uzhinsky[1,5], D. H. Wright[6]

1. CERN, Geneve
2. Lebedev Physical Institute, Moscow
3. Ecoanalytica, MSU, Moscow
4. ITEP. Moscow 5. LIT JINR, Dubna
6. SLAC, Stanford

Abstract

An update of the status of the simulation of hadronic shower shapes in GEANT4 for high-energy calorimetry applications, relevant, in particular, for the experiments at the LHC, is shortly described.
This report is a follow up of the studies presented in the note [1].
The main improvements are the inclusion of quasi-elastic scattering, in the high-energy string models, and Bertini cascade. We recommend the Physics List QGSP_BERT for simulations of the LHC experiments.

1 Introduction

Few years ago, it was observed [2] in calorimeter test-beam set-ups for the experiments at the LHC with high-energy pions that GEANT4 [3] simulation produced hadronic showers that were shorter and narrower than the data when the Physics List QGSP was used. The parameterized Physics List LHEP (based on a C++ rewriting of GHEISHA [4] hadronic generator used in Geant3 [5]) produced hadronic showers with longitudinal profiles closer to the data than the theory-driven Physics Lists QGSP, although the latter was superior as far as the energy response (e/π ratio) and energy resolution were concerned.

In order to improve the description of hadronic shower shapes in GEANT4 , a thorough examination of the relevant GEANT4 hadronic physics models have been undertaken. In particular, the following aspects of hadronic physics have been reviewed: inelastic cross-sections; elastic scattering; neutron production and transportation; high-energy string models; nuclear cascade models. In these studies, we have taken a two-fold approach: first, each of these hadronic models have been validated with

thin-target data; second, simplified calorimeters where employed to assess the impact of each model in macroscopic observables relevant for hadronic showers.

We refer the reader to the note [1] for a comprehensive report of these studies.

In this note we give an update of the improvements that have been achieved in the last year and a half concerning the simulation of hadronic shower shapes in GEANT4 for high-energy calorimetry applications, which are relevant to the experiments at the LHC.

The structure of this note is the following.

In section 2 we discuss the quasi-elastic interactions, whose revision has been essential to the improvement of longitudinal hadronic shower shapes. In section 3 we present the Physics List QGSP_BERT, which is the current recommended one to be used for physics analysis of the experiments at the LHC. In section 4 we demonstrate the improvements of the hadronic shower profiles. A more detailed example will be shown in the Appendix. In section 5 we present the progress on the Fritiof model in GEANT4 , and few interesting Physics Lists that make use of it. Finally, we conclude and discuss some directions of further research.

2 Quasi-elastic scattering of hadrons on nuclei

Three processes are usually distinguished in the theory of high-energy hadron scattering on nuclei: elastic scattering, when the recoil nucleus is left in its ground state; quasi-elastic scattering, when the recoil nucleus is left in an excited state; multiparticle production, when new particles are produced in the interaction. The elastic scattering is a coherent process, involving the entire nucleus; its description requires the calculation of an amplitude or to use some parameterization. The quasi-elastic scattering process is treated as a multiple elastic scattering of the projectile on nuclear nucleons (charge-exchange of the projectile is important only at intermediate and low energies). This process leaves the nucleus in an excited state, which then evolves into its ground state by emitting, in most cases, some nucleons and gammas. Therefore, quasi-elastic scattering is an inelastic hadronic process.

In GEANT4 , up to version 8.2, the quasi-elastic cross-section was included in the inelastic cross-section, but its final state was not properly simulated in the high-energy string models. Instead of the correct final state, it was simulated as multiparticle production, that resulted in an over-production of particles, which caused the simulated hadronic showers to start too early and be shorter than in the data.

Starting with GEANT4 version 8.3 (released in May 2007), a separate quasi-elastic scattering channel was included in high-energy models only. In this implementation, the fraction of the inelastic interactions associated to quasi-elastic scattering is calculated; then, if selected, a corresponding final state is generated. This is modeled as an elastic scattering on a single nucleon, which is the dominant contribution on most of the nuclei.

The inclusion of quasi-elastic scattering in QGS-based Physics Lists (notably QGSP and QGSP_BERT) produces longer hadronic showers. These have been shown to be in better agreement with test-beam data [8], [9].

Note that for calorimeters made of Copper as absorber, the effect of longer showers is almost negligible, due to a cancellation with another change, *i.e.* the increase of 4% of the inelastic pion-Copper cross-section. The latter was made in order to bring it back to the measured value (in GEANT4 version 7.0 and later, it was reduced as a first attempt to improve the shower shapes).

After the first release of quasi-elastic scattering in GEANT4 , users reported three problems:

- An unexpectedly sharp peak near 0 degrees in the angular distribution of protons, produced by the collisions of proton beam particles with kinetic energy of 29 GeV on a Copper target, was reported by the NA61 Collaboration. This was due to an error on the implementation of the angular distribution of proton-proton elastic scattering, fixed in GEANT4 version 9.1.p02.

- "Strange" angular distributions, with a peak at around 70°, of secondary particles produced by the collisions of protons and pions with beryllium nuclei at energies of 8-9 GeV were reported in a recent paper by the HARP-CDP group [6]. This was caused by neglecting the Fermi motion in the simulation of the quasi-elastic scattering, which has been fixed in GEANT4 version 9.1.p02.

- In the same HARP-CDP paper mentioned in the previous item, it appeared some unreasonably diffraction-like patterns in the angular distributions of secondary particles. These were caused by an incorrect sampling of few kinematic variables, as inherited from the GHEISHA model. This has been fixed in GEANT4 version 9.1.p03.

3 Physics List QGSP_BERT

The inclusion of Bertini cascade model to the QGSP Physics List, named QGSP_BERT Physics List, produces hadronic showers significantly wider, in better agreement with test-beam data. The model also contributes to make showers longer, but not enough unless quasi-elastic scattering is properly simulated. This happened starting with GEANT4 version 8.3 (released in May 2007). Preliminary test-beam results (not yet published, but reported in various presentations in [7], in particular see [8] and [9]) indicate that pion showers are well described by QGSP_BERT with GEANT4 version 8.3, or newer.

The Physics List QGSP_BERT comprises the following hadronic models:

- Quark Gluon String (QGS) model for pions, kaons, neutrons, and protons interactions with nuclei at energies above 12 GeV, followed by:

Precompound (P) model for precompound and evaporation phases of the residual nucleus;

- Low-Energy Parameterized (LEP) model for pions, kaons neutrons, and protons interactions with nuclei at energies between 9.5 GeV and 25 GeV;
  for low-energy neutrons, also the parameterized capture and fission is used;

- Bertini (BERT) cascade model, which includes intra-nuclear cascade, followed by precompound and evaporation phases of the residual nucleus, for pions, kaons, neutrons, and protons interactions with nuclei at energies below 9.9 GeV;
  (note that Bertini model is not applied for rescattering of secondary hadrons inside the nucleus produced by QGS)

- parameterized (LEP + HEP) models for all remaining hadrons (*i.e.* hyperons).

Note that in the overlapping regions between models (*e.g.* 12-25 GeV for LEP and QGS; 9.5-9.9 GeV for Bertini and LEP), a random sampling is performed to decide for each interaction which of the two models to use, according to a linear energy dependency of the corresponding probabilities in the overlapping region (*e.g.* 100% LEP model at 12 GeV; 100% QGS model at 25 GeV).

In the next section an example will show the improvements on the shower shapes for incident pions obtained with the Physics List QGSP_BERT starting with version 8.3.

For protons, QGSP_BERT showers are still fairly shorter than observed in the data. We suspect that the main cause might be due to the diffraction process. In fact, preliminary benchmarks of this model with thin-target data seems to confirm the inadequateness of the current implementation.

Some interesting alternative Physics Lists, especially for proton showers, will be presented in section 5.

Overall, taking into account also the energy response and energy resolution, the Physics List QGSP_BERT is our current recommended Physics List for physics analysis for the experiments at the LHC.

4 Improvements on hadronic shower shapes

We show here an example of the GEANT4 improvements in the simulation of hadronic shower profiles, discussed in the two previous sections. We considered π^- beam particles with kinetic energy of 100 GeV impinging on two types of simplified cylindrical hadronic calorimeters:

- 60 layers of 25 mm Copper absorber and 8.5 mm Liquid Argon active material;

- 100 layers of 17 mm Iron absorber and 4 mm plastic Scintillator.

The size of these calorimeters is equivalent to about 10 λ (*i.e.* interaction lengths) in depth and diameter. No quenching effects have been included: their impact on hadronic shower profiles is small (whereas it would be relevant for the energy response in the case of Scintillators).

To summarize the longitudinal shower development, we consider the following four observables:

- f_{L1} : fraction of the visible energy in the first longitudinal quarter of the calorimeter (*i.e.* in the first 2.5 λ);
- f_{L2} : fraction of the visible energy in the second longitudinal quarter of the calorimeter (*i.e.* in the region 2.5 - 5.0 λ);
- f_{L3} : fraction of the visible energy in the third longitudinal quarter of the calorimeter (*i.e.* in the region 5.0 - 7.5 λ);
- f_{L4} : fraction of the visible energy in the last (fourth) longitudinal quarter of the calorimeter (*i.e.* in the region 7.5 - 10 λ).

Similarly, to summarize the lateral shower development, we consider the following 3 observables:

- f_{R1} : fraction of the visible energy in the first radial ring, defined as a radius less than 0.4 λ from the beam direction;
- f_{R2} : fraction of the visible energy in the second radial ring, defined as a radius between 0.4 - 1.2 λ from the beam direction;
- f_{R3} : fraction of the visible energy in the last (third) radial ring, defined as a radius above 1.2 λ from the beam direction.

By definition, $f_{L1} + f_{L2} + f_{L3} + f_{L4} = 1$, and $f_{R1} + f_{R2} + f_{R3} = 1$.
To give an example of the physical meaning of these variables, compact hadronic showers have larger f_{L1}, f_{L2}, f_{R1}, and smaller f_{L3}, f_{L4}, f_{R2}, f_{R3} .

We consider here three versions of GEANT4 : 8.2.p01, as an example of a release before the inclusion of quasi-elastic scattering; 8.3.p02 and 9.1.p02 as examples of newer versions widely used by the experiments at the LHC. As Physics Lists, we present LHEP (the parameterized one that provides a good description of longitudinal showers), QGSP (the one mostly used in the past by the experiments at the LHC), and QGSP_BERT (the current default one used by the experiments ATLAS and CMS). Furthermore, to better study the effect of the quasi-elastic scattering, we consider also the special Physics Lists QGSP_NQE and QGSP_BERT_NQE, that are identical to QGSP and QGPS_BERT, respectively, except that quasi-elastic scattering is not included ("NQE" stands for "No Quasi-Elastic"). These Physics Lists, introduced in GEANT4 version 8.3, are meant only for studies of the effect of the recent changes.

From the results showed in the tables 1 and 2 we can make the following observations:

- Comparing the Physics Lists QGSP against QGSP_NQE (or similarly QGSP_BERT against QGSP_BERT_NQE), it demonstrates that the inclusion of quasi-elastic scattering makes hadronic showers significantly longer. In each comparison, we keep constant the version of Geant4 (8.3.p02 or 9.1.p02).

- Comparing the same Physics List between GEANT4 version 8.2.p01 and either 8.3.p02 or 9.1.p02, one sees that hadronic showers become longer in QGS-based Physics Lists in the case of an Iron - Scintillator calorimeter, but not for a Copper - Liquid Argon calorimeter (due to the change of the inelastic pion-Copper cross-section, as explained in section 2).

- The inclusion of Bertini cascade model makes hadronic showers longer and significantly wider.

- Differences on the hadronic shower shapes between the GEANT4 versions 8.3.p02 and 9.1.p02 are minor (these are due to some improvements in the Bertini and Precompound/Evaporation models).

In the Appendix we will show other observables of interest in high-energy calorimetry, including also other Physics Lists that we are going to define in the next section.

We conclude this section with two plots from the ATLAS Hadron End-Cap (HEC) test-beam [8], a Copper - Liquid Argon calorimeter, that show the progress in the GEANT4 simulation of hadronic shower profiles. Figures 1 and 2 show the ratio between GEANT4 simulations and data on the fraction of visible energy in the four longitudinal compartments, for π^- beam particles of various energies.

G4 8.2.p01	LHEP		QGSP		QGSP_BERT
f_{L1}	53.4%		56.9%		53.6 ± 0.3 %
f_{L2}	34.0%		32.7%		33.6 ± 0.2 %
f_{L3}	10.2%		8.6%		10.3 ± 0.1 %
f_{L4}	2.4%		1.9%		2.4 ± 0.05 %
f_{R1}	76.3%		79.0%		70.3 ± 0.2 %
f_{R2}	20.6%		18.6%		22.9 ± 0.1 %
f_{R3}	3.1%		2.5%		6.8 ± 0.03 %
G4 8.3.p02	LHEP	QGSP_NQE	QGSP	QGSP_BERT_NQE	QGSP_BERT
f_{L1}	53.0%	59.5%	57.6%	54.9%	52.7%
f_{L2}	34.5%	31.2%	31.8%	32.9%	33.6%
f_{L3}	10.2%	7.7%	8.8%	10.0%	10.9%
f_{L4}	2.3%	1.7%	1.8%	2.2%	2.7%
f_{R1}	75.2%	78.9%	78.9%	70.5%	70.5%
f_{R2}	21.5%	18.6%	18.6%	22.7%	22.7%
f_{R3}	3.3%	2.5%	2.5%	6.8%	6.8%
G4 9.1.p02	LHEP	QGSP_NQE	QGSP	QGSP_BERT_NQE	QGSP_BERT
f_{L1}	53.2%	59.3%	57.0%	55.0%	54.0%
f_{L2}	34.4%	31.3%	32.0%	32.8%	33.1%
f_{L3}	10.0%	7.8%	9.0%	9.9%	10.3%
f_{L4}	2.4%	1.6%	2.0%	2.3%	2.6%
f_{R1}	75.3%	79.1%	78.8%	70.9%	71.0%
f_{R2}	21.4%	18.4%	18.7%	22.7%	22.6%
f_{R3}	3.3%	2.5%	2.5%	6.4%	6.4%

Table 1: π^- beam particles with kinetic energy of 100 GeV impinging on a Copper - Liquid Argon calorimeter. The errors in the last column of the top part of the table correspond to the statistical uncertainties obtained with 5000 simulated primary tracks.

G4 8.2.p01	LHEP		QGSP		QGSP_BERT
f_{L1}	49.0%		55.7%		51.7 ± 0.3 %
f_{L2}	36.3%		33.6%		34.9 ± 0.2 %
f_{L3}	11.9%		8.9%		10.8 ± 0.1 %
f_{L4}	2.8%		1.8%		2.6 ± 0.06 %
f_{R1}	74.3%		76.8%		64.2 ± 0.2 %
f_{R2}	22.2%		20.5%		28.1 ± 0.1 %
f_{R3}	3.5%		2.7%		7.6 ± 0.02 %
G4 8.3.p02	LHEP	QGSP_NQE	QGSP	QGSP_BERT_NQE	QGSP_BERT
f_{L1}	50.0%	57.1%	55.3%	52.4%	50.4%
f_{L2}	35.8%	32.2%	33.3%	34.5%	34.8%
f_{L3}	11.5%	8.8%	9.3%	10.6%	11.6%
f_{L4}	2.7%	1.9%	2.1%	2.5%	3.2%
f_{R1}	73.2%	76.6%	76.5%	64.4%	64.4%
f_{R2}	23.1%	20.7%	20.8%	28.1%	28.0%
f_{R3}	3.7%	2.7%	2.7%	7.5%	7.5%
G4 9.1.p02	LHEP	QGSP_NQE	QGSP	QGSP_BERT_NQE	QGSP_BERT
f_{L1}	49.9%	56.1%	54.2%	51.4%	48.8%
f_{L2}	36.1%	33.5%	34.4%	34.9%	35.8%
f_{L3}	11.4%	8.6%	9.3%	11.1%	12.1%
f_{L4}	2.6%	1.8%	2.1%	2.6%	3.3%
f_{R1}	73.1%	76.7%	76.8%	65.4%	65.2%
f_{R2}	23.2%	20.7%	20.6%	27.6%	27.8%
f_{R3}	3.7%	2.6%	2.6%	7.0%	7.0%

Table 2: π^- beam particles with kinetic energy of 100 GeV impinging on an Iron - Scintillator calorimeter. The errors in the last column of the top part of the table correspond to the statistical uncertainties obtained with 5000 simulated primary tracks.

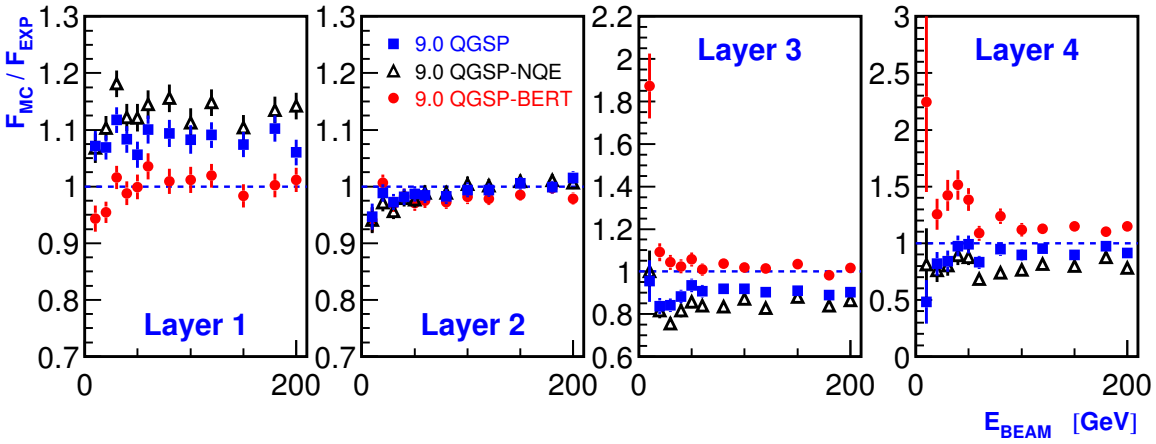

Figure 1: Ratio between GEANT4 version 9.0 simulations and experimental data on the fractions of visible energy in the four longitudinal sections of the ATLAS HEC (Cu-LAr) calorimeter test-beam set-up, for π^- beam particles of various energies. The Physics List QGSP_BERT provides hadronic showers that are longer than the ones obtained with the Physics List QGSP, in better agreement with experimental data.

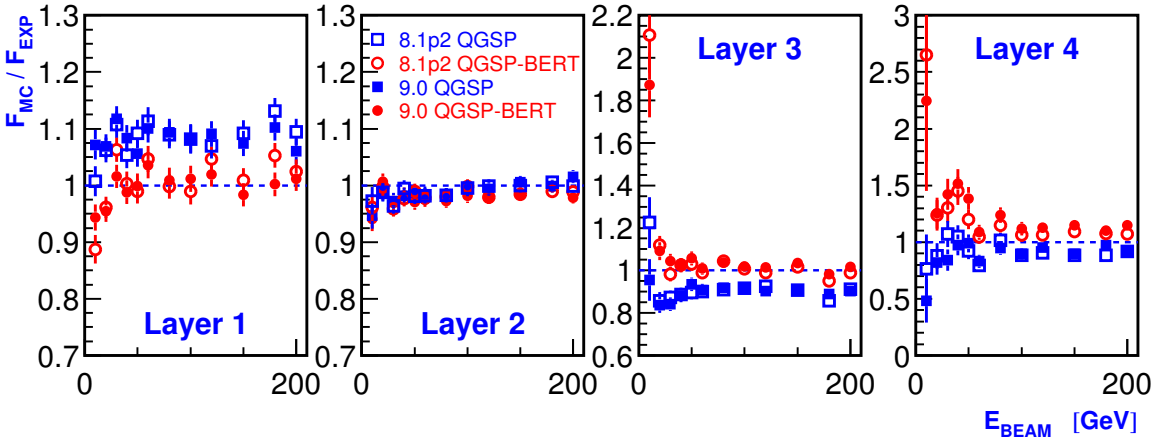

Figure 2: Ratio between GEANT4 simulations, with versions 8.1.p02 and 9.0, and experimental data on the fractions of visible energy in the four longitudinal sections of the ATLAS HEC (Cu-LAr) calorimeter test-beam set-up, for π^- beam particles of various energies. There are no significant differences between the GEANT4 versions 8.1.p02 and 9.0, due to the compensation between quasi-elastic scattering and change in pion-Copper cross-section.

5 Fritiof model

The Quark-Gluon String (QGS) model is based on the high-energy reggeon phenomenology, and, due to this, it has some problems at sufficiently low energies. First of all, the applied asymptotical Abramovski-Kancheli-Gribov cutting rules have to be corrected. The treatment of the diffraction dissociation processes requires a special consideration. Non-vacuum exchanges that are very important at low energies must be taken into account. Three reggeon interactions have to be properly included in order to provide a smooth transition from high to low energies, and so on. Most of the questions are not solved until now. Thus there is no program implementation of the QGS model which is correct from a theoretical point of view. At the same time a simpler phenomenological approach based on the wounded nucleon model is applied quite successfully at high energies. This is implemented in UrQMD, HSD, ART and HIJING models originated from the FRITIOF model [10].

The well-known FRITIOF model is implemented in GEANT4 under the abbreviation FTF [11]. It allows to simulate the quasi-elastic scattering and the diffraction processes. The quasi-elastic scattering is treated, as in all cascade models, without taking into account Fermi-momentum dependence on nuclear density (a constant value of $\sim 200\, MeV/c$ is used as Fermi-momentum). For the simulation of the diffraction dissociation the original Fritiof algorithm is used. In this model the cross section of the process decreases rapidly as energy grows, in disagreement with known experimental data. We have tuned the cross section behaviour of the diffraction dissociation as a function of the energy to agree with experimental data, and we have simulated the processes separately from other inelastic hadron-nucleon interactions. This decreases the multiplicity of produced particles, and increases the shower length a little bit.

It is very important that the parameterized cross section of the diffraction dissociation increases towards the hadron-nucleon inelastic cross section as the energy decreases. Thus, the diffraction processes dominate in hadron-nucleus interactions at energies of the order of 3–10 GeV. These diffraction processes look like resonance production and penetration in nuclei, and therefore they provide a smooth transition from high to low energies, and a natural connection with the low-energy GEANT4 models.

The FTF model can be used now for simulating hadron-hadron and hadron-nucleus interactions starting from laboratory momenta of 4–5 GeV/c. A significant effort has been spent in order to tune the model parameters for a better description of hadron-nucleon interactions. As a result, the model describes particle spectra better than several other known models, like HIJING, UrQMD, and QGS [12].

A recent upgrade of the FTF model in GEANT4 includes also a treatment of the secondary particle formation time, which is required for any coupling with low-energy cascade models. This is needed to simulate slow particle cascading in residual nuclei. Now a combination of the FTF and Binary cascade models gives a quite satisfactory

result for hadron-nucleus interactions, especially in the case of HARP experimental data.

Between the GEANT4 Physics Lists that use Fritiof, two look particularly interesting because of their reduced usage of parameterized models:

FTF_BIC which comprises the following hadronic models:

- Fritiof (FTF) model for pions, kaons, neutrons, and protons interactions with nuclei at energies above 4 GeV;
- Binary (BIC) cascade model, which includes: rescattering of secondary pions, neutrons and protons inside the nucleus, followed by precompound and evaporation phases of the residual nucleus, for primary pions, kaons, neutrons and protons interactions with nuclei at energies above 4 GeV;
  for primary pions, neutrons and protons interactions with nuclei at energies below 5 GeV, BIC includes intra-nuclear cascade, followed by precompound and evaporation phases of the residual nucleus;
- Low-Energy Parameterized (LEP) model for kaons interactions with nuclei with energies below 5 GeV;
  for low-energy neutrons, the parameterized capture and fission is also used;
- parameterized (LEP + HEP) models for all remaining hadrons (*i.e.* hyperons).

FTFP_BERT which comprises the following hadronic models:

- Fritiof (FTF) model for pions, kaons, neutrons, and protons interactions with nuclei at energies above 4 GeV, followed by:
  Precompound (P) model for precompound and evaporation phases of the residual nucleus;
- Bertini (BERT) cascade model, which includes intra-nuclear cascade, followed by precompound and evaporation phases of the residual nucleus, for pions, kaons, neutrons, and protons interactions with nuclei at energies below 5 GeV;
  (note that the Bertini model is not used for rescattering of secondary hadrons inside the nucleus produced by FTF)
- parameterized models for low-energy neutron capture and fission;
- parameterized (LEP + HEP) models for all remaining hadrons (*i.e.* hyperons).

Note that in the overlapping regions between models (*e.g.* 4-5 GeV for BIC/BERT/LEP and FTF), a random number is drawn to decide for each interaction which of the two models to use, according to a linear rule (*e.g.* 100% BIC/BERT/LEP at 4 GeV; 100% FTF at 5 GeV).

In the Appendix, the tables 3 and 4 show an example of the comparison of these Physics Lists with others, in the case, respectively, of π^- and proton beam particles with kinetic energy of 100 GeV impinging on a Copper-Liquid Argon calorimeter. Note in particular that FTF_BIC and FTF_BERT Physics Lists produce longer showers for incident protons than QGSP_BERT, in better agreement with test-beam data [13].

6 Conclusions

In this note we have presented an update of the status of the simulation of hadronic shower shapes in GEANT4 . The main conclusions are the following.

Starting with GEANT4 version 8.3 (released in May 2007), the QGSP_BERT Physics List provides a good description of both longitudinal and lateral shower profiles for incident pions. The energy response (e/π ratio) and energy resolution are also reasonably described by this Physics List. As a result, we recommend it for physics simulations of the LHC experiments.

The longitudinal shower profile for protons for the Physics List QGSP_BERT is still fairly shorter than data, most likely due to an inaccurate modelling of diffraction. We are benchmarking this process with published data.

The Fritiof model in GEANT4 has been significantly improved in the latest release 9.2.b01 and the two Physics Lists FTF_BIC and FTFP_BERT could be considered as promising alternatives to QGSP_BERT, in particular for the longitudinal profile of protons. Another interesting feature of these Physics Lists is that the use of parameterized models is limited to low-energy neutron capture and fission (and, in the case of FTF_BIC, for kaons interactions with energy below 5 GeV), and for hyperons. This implies fewer transitions between hadronic models, and an improved conservation of energy.

7 Open issues

Now that the hadronic shower shapes are reasonably well simulated by at least some Physics Lists in GEANT4 , what appears to require more urgent study and improvement in the description of hadronic showers in GEANT4 are the energy response and energy resolution. In particular, by studying these observables as a function of the beam energy, from few GeV up to hundreds of GeV, a non-smooth behaviour is seen in correspondence of the transitions between hadronic models. The experiments ATLAS [13] and CMS [14] have reported instances of these discontinuities in their calorimeter test-beam setups, and preliminary studies in simple set-ups have confirmed them.
Another problem under investigation is the higher energy response of FTF-based Physics Lists.

8 Appendix: comparison between GEANT4 Physics Lists

Tables 3 and 4 show the comparison of some GEANT4 Physics Lists for the following observables (defined in [1], but rewritten explicitly here for the readers' convenience):

- E_{vis} : the average visible energy, *i.e.* the sum of the energies deposited in each active layer;
- E_{tot} : the average total energy deposited in the whole calorimeter;
- σ_E/E : energy resolution; the notation is a shorthand for precisely: $\sigma_{E_{vis}}/E_{vis}$;
- e/π : ratio between the average visible energy for an electron beam, and the average visible energy for a pion beam of the same energy;
  (similarly, e/p for a proton beam)
- f_{L1}, ... f_{L4} : fractions of the visible energy in each longitudinal quarter of the calorimeter;
- f_{R1}, f_{R2}, f_{R3} : fractions of the visible energy in three radial rings of increasing radius (distance) with respect to the beam direction;
- *exit_kin* : the exiting kinetic energy per event, *i.e.* the average sum of the kinetic energies of all tracks exiting the calorimeter in an event;
  we consider also the fraction of the exiting kinetic energy which is due to some particle types, *e.g.* neutrons, gammas, neutrinos, muons, etc, and the average number of these tracks per event; we will use later the following two variables:
  - *exit_fn* : fraction of the exiting kinetic energy due to neutrons;
  - *exit_#n* : average number of exiting neutrons per event;
- the average number of created tracks (and steps as well) per event, for different particle types; in particular, we will use the following variables:
  - $\#EM$: average number of electron, positron, and gamma tracks per event;
  - $\#\pi$: average number of pion (neutral and charged) tracks per event;
  - π^0/π : ratio between the average number of neutral pion tracks and the average number of pion (neutral and charged) tracks;
  - $\#p$: average number of proton tracks per event;
  - $\#n$: average number of neutron tracks per event;
- the average track length inside the calorimeter, for different particle types; we will use the following variable:

- L_n : average track length for neutrons (fully inside the calorimeter);

- the visible energy contribution, total, layer by layer, ring by ring, of different particle types (electrons/positrons; muons; charged pions; charged kaons; protons/antiprotons; neutrons/ions: note that we group together neutrons and ions because, since GEANT4 version 8.1, neutrons can deposit energy, which corresponds physically to elastic recoiled nuclei with kinetic energies below a certain threshold, currently fixed at 100 keV, without producing the secondary).

The results reported in the tables 3 and 4 refer to the case of negative pion and proton beam particles, respectively, with kinetic energies of 100 GeV impinging on a simplified cylindrical Copper - Liquid Argon calorimeter. The size of the calorimeter is equivalent to about 10 λ (*i.e.* interaction lengths) in depth and diameter. 5000 events (*i.e.* primary tracks) have been simulated. We use GEANT4 version 9.2.b01.

Observable	LHEP	QGSP	QGSP_BERT	FTF_BIC	FTFP_BERT
E_{vis}	3881 ± 5 MeV	4101	4488	4607	4564
σ_E/E	9.2%	8.1%	5.3%	5.5%	5.0%
e/π	1.24	1.18	1.07	1.05	1.06
f_{L1}	52.6 ± 0.3 %	57.7%	53.3%	52.8%	53.2%
f_{L2}	34.9 ± 0.2 %	31.8%	33.9%	34.1%	33.3%
f_{L3}	10.1 ± 0.1 %	8.4%	10.3%	10.5%	10.7%
f_{L4}	2.4 ± 0.06 %	2.1%	2.5%	2.6%	2.8%
f_{R1}	75.5 ± 0.2 %	79.1%	71.0%	71.5%	72.0%
f_{R2}	21.3 ± 0.1 %	18.4%	22.6%	22.8%	22.2%
f_{R3}	3.2 ± 0.02 %	2.5%	6.4%	5.6%	5.8%
$\#EM$	95,162 ± 348	111,698	139,563	146,781	143,215
$\#\pi$	133 ± 0.3	113	104	113	101
π^0/π	38%	38%	32%	32%	33%
$\#p$	446 ± 2	404	420	325	381
$\#n$	764 ± 3	746	2135	1741	1951
L_n	141 ± 0.1 mm	298	722	680	726
exit_kin	3077 ± 71 MeV	2653	2404	2973	2473
exit_fn	17 ± 0.5 %	13%	19%	15%	17%
exit_#n	61 ± 0.3	15	89	69	80
e_E_{vis}	65.6%	72.3%	72.9%	75.1%	74.6%
e_f_{L1}	55.7%	61.4%	57.8%	56.7%	57.5%
e_f_{L2}	33.4%	29.8%	31.7%	32.3%	31.1%
e_f_{L3}	8.8%	7.1%	8.6%	9.0%	9.1%
e_f_{L4}	2.1%	1.7%	1.9%	2.0%	2.3%
e_f_{R1}	81.5%	84.6%	76.9%	77.3%	78.1%
e_f_{R2}	16.6%	13.9%	17.3%	17.8%	16.7%
e_f_{R3}	2.0%	1.5%	5.8%	4.9%	5.1%
p_E_{vis}	15.7%	12.9%	14.4%	12.9%	13.1%
p_f_{L1}	45.5%	46.4%	39.2%	37.6%	38.2%
p_f_{L2}	38.2%	38.2%	41.0%	41.2%	40.7%
p_f_{L3}	13.1%	12.4%	15.7%	16.6%	16.3%
p_f_{L4}	3.3%	3.1%	4.2%	4.7%	4.8%
p_f_{R1}	55.9%	57.9%	52.7%	48.8%	50.6%
p_f_{R2}	35.3%	34.8%	39.0%	41.5%	41.3%
p_f_{R3}	8.8%	7.3%	8.3%	9.7%	8.1%
π_E_{vis}	10.9%	8.7%	9.6%	9.3%	9.2%
π_f_{L1}	47.0%	50.1%	45.5%	45.7%	44.5%
π_f_{L2}	37.9%	36.0%	38.3%	37.7%	38.0%
π_f_{L3}	12.1%	11.2%	13.0%	13.1%	13.7%
π_f_{L4}	3.0%	2.7%	3.2%	3.5%	3.8%
π_f_{R1}	73.7%	74.5%	63.9%	63.8%	62.8%
π_f_{R2}	24.6%	24.0%	31.9%	32.6%	33.2%
π_f_{R3}	1.7%	1.5%	4.1%	3.7%	4.0%
n_E_{vis}	7.2%	5.4%	2.5%	2.0%	2.2%
n_f_{L1}	49.6%	48.5%	38.9%	40.0%	37.4%
n_f_{L2}	36.1%	36.9%	40.5%	39.7%	40.6%
n_f_{L3}	11.3%	11.8%	16.3%	15.8%	17.1%
n_f_{L4}	3.0%	2.8%	4.3%	4.6%	4.9%
n_f_{R1}	66.8%	65.6%	35.8%	39.0%	34.5%
n_f_{R2}	28.1%	29.4%	44.5%	43.5%	45.5%
n_f_{R3}	5.1%	5.1%	19.7%	17.4%	19.9%
k_E_{vis}	0.3%	0.4%	0.3%	0.5%	0.5%
μ_E_{vis}	0.2%	0.2%	0.2%	0.2%	0.2%

Table 3: Comparisons between GEANT4 Physics Lists, for π^- beam particles with kinetic energy of 100 GeV impinging on a Copper-Liquid Argon calorimeter.

Observable	LHEP	QGSP	QGSP_BERT	FTF_BIC	FTFP_BERT
E_{vis}	3779 ± 4 MeV	3976	4433	4576	4497
σ_E/E	8.1%	7.3%	5.0%	5.4%	4.8%
e/π	1.28	1.21	1.09	1.05	1.07
f_{L1}	54.6 ± 0.3 %	63.0%	57.8%	53.4%	52.9%
f_{L2}	33.8 ± 0.2 %	29.2%	31.8%	34.1%	34.5%
f_{L3}	9.6 ± 0.1 %	6.7%	8.6%	10.1%	10.2%
f_{L4}	2.0 ± 0.05 %	1.2%	1.8%	2.4%	2.3%
f_{R1}	73.3 ± 0.2 %	75.5%	66.5%	64.7%	65.3%
f_{R2}	23.2 ± 0.1 %	21.5%	26.0%	28.1%	27.3%
f_{R3}	3.5 ± 0.02 %	2.9%	7.5%	7.2%	7.4%
$\#EM$	86,545 ± 250	99,315	132,475	138,881	133,731
$\#\pi$	140 ± 0.3	129	118	136	122
π^0/π	38%	39%	32%	32%	33%
$\#p$	496 ± 1	484	500	423	485
$\#n$	844 ± 3	885	2511	2225	2457
L_n	141 ± 0.1 mm	294	712	674	720
exit_kin	3291 ± 57 MeV	2662	2448	3234	2665
exit_fn	21 ± 0.8 %	16%	22%	18%	20%
exit_#n	68 ± 0.3	21	114	92	105
e_E_{vis}	61.3%	66.2%	67.9%	68.4%	67.8%
e_f_{L1}	58.1%	67.3%	62.7%	57.7%	57.5%
e_f_{L2}	32.0%	26.4%	28.9%	31.9%	32.1%
e_f_{L3}	8.3%	5.4%	7.1%	8.5%	8.6%
e_f_{L4}	1.6%	0.9%	1.4%	1.8%	1.9%
e_f_{R1}	78.7%	81.0%	71.9%	70.0%	71.1%
e_f_{R2}	19.0%	17.0%	20.7%	23.2%	21.6%
e_f_{R3}	2.2%	2.0%	7.4%	6.8%	7.2%
p_E_{vis}	18.7%	16.6%	17.9%	17.3%	17.7%
p_f_{L1}	47.7%	53.3%	45.8%	41.7%	41.7%
p_f_{L2}	37.3%	35.4%	38.9%	39.8%	40.4%
p_f_{L3}	12.3%	9.5%	12.5%	14.7%	14.3%
p_f_{L4}	2.8%	1.8%	2.8%	3.9%	3.6%
p_f_{R1}	58.0%	59.6%	54.1%	50.4%	51.5%
p_f_{R2}	33.7%	33.6%	38.0%	40.2%	40.5%
p_f_{R3}	8.3%	6.7%	7.9%	9.4%	8.0%
π_E_{vis}	11.2%	9.7%	10.6%	10.9%	10.8%
π_f_{L1}	49.2%	56.2%	51.2%	48.3%	46.7%
π_f_{L2}	37.3%	33.8%	36.4%	37.6%	38.3%
π_f_{L3}	11.2%	8.4%	10.2%	11.5%	12.2%
π_f_{L4}	2.4%	1.5%	2.2%	2.6%	2.8%
π_f_{R1}	73.4%	72.9%	61.7%	61.0%	59.9%
π_f_{R2}	25.1%	25.7%	34.0%	35.0%	35.8%
π_f_{R3}	1.5%	1.5%	4.3%	4.0%	4.3%
n_E_{vis}	8.1%	6.6%	2.9%	2.5%	2.8%
n_f_{L1}	52.7%	55.2%	44.3%	42.7%	41.1%
n_f_{L2}	34.3%	34.0%	39.5%	39.2%	40.4%
n_f_{L3}	10.7%	9.1%	13.2%	14.3%	14.7%
n_f_{L4}	2.3%	1.6%	3.1%	3.8%	3.7%
n_f_{R1}	68.3%	66.2%	35.7%	38.5%	34.7%
n_f_{R2}	26.8%	28.8%	44.3%	44.0%	45.2%
n_f_{R3}	4.9%	5.0%	20.0%	17.5%	20.1%
k_E_{vis}	0.4%	0.4%	0.4%	0.6%	0.6%
μ_E_{vis}	0.3%	0.2%	0.2%	0.3%	0.2%

Table 4: Comparisons between GEANT4 Physics Lists, for proton beam particles with kinetic energy of 100 GeV impinging on a Copper-Liquid Argon calorimeter.

References

[1] J. Apostolakis, G. Folger, V. Grichine, A. Howard, V. Ivanchenko, M. Kosov, A. Ribon, *"Hadronic Shower Shape Studies in* GEANT4 *"*, CERN-LCGAPP-2007-02, available at http://lcgapp.cern.ch/project/mgmt/doc.html

[2] F. Gianotti *et al.*, *"*GEANT4 *hadronic physics validation with LHC test-beam data: first conclusions"*, CERN-LCGAPP-2004-10, available at http://lcgapp.cern.ch/project/mgmt/doc.html

[3] S. Agostinelli *et al.*, GEANT4 Collaboration, *"*GEANT4 *- a simulation toolkit"*, Nuclear Instruments and Methods in Physics Research, A 506 (2003) 250. J. Allison *et al.*, *"*GEANT4 *developments and applications",* IEEE Transactions on Nuclear Science 53 No. 1 (2006) 270-278. See also the GEANT4 web page: http://cern.ch/geant4

[4] H. Fesefeld, *"Simulation of hadronic showers, physics and applications"*, Technical Report PITHA 85-02, Aachen, Germany, Sept. 1985.

[5] R. Brun, F. Carminati, S. Giani, *"GEANT detector description and simulation"*, Program Library Long Writeup W5013, 1994, CERN.

[6] A. Bolshakova *et al.*, HARP-CDP Collaboration, Eur.Phys.J.C56:323-332,2008, arXiv:0804.3013v1

[7] Web page of "LCG Physics Validation for LHC Simulations": http://lcgapp.cern.ch/project/simu/validation

[8] A. Kiryunin and P. Strizenec, presentation at the LCG Physics Validation meeting, on 17 October 2007, available at http://indico.cern.ch/conferenceDisplay.py?confId=21884

[9] T. Carli and M. Simonyan, presentation at the LCG Physics Validation meeting, on 17 October 2007, available at http://indico.cern.ch/conferenceDisplay.py?confId=21884

[10] B. Andersson, G. Gustafson, and B. Nielsson-Almquist, *"A model for low-pT hadronic reactions with generalizations to hadron-nucleus and nucleus-nucleus collisions"*, Nucl. Phys. 281 (1987) 289; see also B. Nilsson-Almquist and E. Stenlund, Comp. Phys. Commun. 43 (1987) 387.

[11] V. Uzhinsky, *"Fritiof model in* GEANT4 *"*,
to appear in the proceedings of the IEEE conference, Dresden, 19–25 October 2008.

[12] G. Folger and V. Uzhinsky, *"Validation of high-energy models in* GEANT4 *"*,
to appear in the proceedings of the IEEE conference, Dresden, 19–25 October 2008.

[13] T. Carli and M. Simonyan, presentation at the LCG Physics Validation meeting, on 24 September 2008, available at http://indico.cern.ch/conferenceDisplay.py?confId=39762

[14] S. Piperov, presentation at the LCG Physics Validation meeting, on 7 May 2008, available at http://indico.cern.ch/conferenceDisplay.py?confId=31702